

Low-activity ^{125}I implantation into VX₂ tumor rabbits and quantitative evaluation of the precise therapeutic effect

ZHENG WANG, JUAN WANG, YONGYI YAO, FENG WANG, QIANG FAN and RUIFENG ZHAO

Department of Nuclear Medicine, Jincheng Anthracitic Coal Mining Group
General Hospital, Jincheng, Shanxi 048006, P.R. China

Received August 14, 2020; Accepted August 18, 2021

DOI: 10.3892/etm.2021.10873

Abstract. There is still controversy about quantitatively evaluating the therapeutic effect of radioactive low-activity iodine-125 seeds (^{125}I seeds). In the present study, a paired VX₂ tumor model in a rabbit hind leg muscle was established, which is virus-induced anaplastic squamous cell carcinoma characterized by hypervascularity, rapid growth and easy propagation in the skeletal muscle. ^{125}I seeds with 0.4 and 0.7 mCi activity were implanted into the left and right legs, respectively, using a radiation treatment planning system under positron emission tomography (PET)/computed tomography (CT) guidance. PET/CT scans and hematoxylin and eosin staining were observed at 72 h and 2 and 4 weeks after implantation to assess the therapeutic effect. The results showed that the average tumor length and standard uptake value (SUV) decreased over time, and both ^{125}I seed groups achieved therapeutic effects at 4 weeks post-implantation. Quantitative evaluation of tumor inhibition rate, SUV variation and tumor marker ratio (Bcl-2/Bax) suggested that 0.7 mCi ^{125}I seeds were more suitable than 0.4 mCi seeds in a clinical setting.

Introduction

Radioactive particle implantation is widely used to treat various types of tumor, such as lung cancer, thoracic esophageal squamous cell carcinoma and hepatocellular carcinoma (1-3), as the ultrastructure of tumor cells can be ruptured and disintegrated by X-rays and γ -rays of radioactive particles within their effective killing radius (4). Low-energy and -dose radioactive ^{125}I seed implantation is a precise radiotherapy technique used for the treatment of malignant tumors, such as hepatocellular carcinoma, lung cancer, head

and neck squamous cell carcinoma and pancreatic cancer. These seeds can be implanted within a close range of the tumor target area with the aid of computer technology that is used to scan and locate the tumor (5). The half-life of ^{125}I is 59.6 days, which is beneficial for clinical applications due to its relatively long half-life and shelf-life (6). However, there is controversy surrounding the quantitative evaluation of ^{125}I seed efficacy, especially in terms of particle activity and the time within which the particle effect is greatest (7,8). To the best of our knowledge, there are few quantitative evaluations that have investigated the therapeutic effect of ^{125}I in precise clinical treatment.

Numerous studies examining the efficacy of ^{125}I seed implantation have been conducted under positron emission tomography (PET)/computed tomography (CT) guidance (9-11); PET/CT images accurately distinguish between surviving tumor cells (characterized by high metabolism of fluorodeoxyglucose) and necrotic areas without metabolism (12).

The standard uptake value (SUV), a mathematically derived ratio of tissue radioactivity concentration and the injected dose of radioactivity per kilogram of patient body weight, is an important semi-quantitative parameter in PET/CT to measure the response of cancer to treatment (13). The tumor inhibition rate can be described as the change in tumor length change before and after treatment (14). Additionally, this pathological parameter can be evaluated using the ratio of Bcl-2/Bax expression levels. Apoptosis and anti-apoptosis imbalance are key processes in tumorigenesis; Bcl-2 serves a role in inhibiting apoptosis and Bax antagonizes Bcl-2 (15,16). The expression levels of Bcl-2 are positively correlated with the degree of tumor malignancy. Therefore, overexpression of Bcl-2 is an important marker for tumor cell development, such as oral and maxillofacial squamous cell carcinoma and colorectal cancer (17,18). The VX₂ tumor cell line, a squamous cell carcinoma derived from rabbit papilloma induced by the ShPoe virus (19), is similar to human tumors, such as lung cancer, in terms of biochemical, biological and morphological characteristics; thus, it has been widely used in clinical research, such as in imaging diagnostics and interventional radiology (20,21).

In the present study, a paired VX₂ tumor model in a rabbit hind leg muscle was established. ^{125}I seeds with 0.4 mCi initial activity were implanted into the left hind legs and seeds with

Correspondence to: Dr Ruifeng Zhao, Department of Nuclear Medicine, Jincheng Anthracitic Coal Mining Group General Hospital, 227 Provincial Road, Beishidian, Jincheng, Shanxi 048006, P.R. China
E-mail: jmzyyzrf@sina.com

Key words: ^{125}I seed implantation, precise therapeutic effect, rabbit VX₂ xenografts, tumor inhibition rate, standard uptake value

0.7 mCi initial activity were implanted into the right hind legs. PET/CT scans were taken before ^{125}I implantation and 72 h and 2- and 4-weeks post-implantation. Changes in tumor length, SUV and the ratio of Bcl-2 to Bax were evaluated. The effectiveness of ^{125}I seeds with different levels of activity were compared and the therapeutic effects were observed. The present study aimed to provide a reference for optimal particle activity and quantitative evaluation of the therapeutic effects of specific, individualized, clinical treatment using the radioactive particle ^{125}I .

Materials and methods

Animal model. New Zealand White rabbits (n=30; age, 3-4 months; weight, 2-3 kg; 15 male and 15 female rabbits) were allowed free access to food and water and housed individually under conditions of 18-26°C, 30-70% relative humidity and a 12/12 h dark/light cycle. All procedures were provided by the Animal Experimental Center of Shanxi Cancer Hospital (Taiyuan, China). The VX_2 tumor block was provided by BeNa Culture Collection; Beijing Beina Chunglian Institute of Biotechnology. The health states of rabbits were recorded every 2 days following implantation. No adverse effects were observed in the animals. The VX_2 solid tumor tissues were cut into ~2 mm³ tumor blocks, resuspended in physiological saline and injected into the bilateral thigh muscles of white rabbits. After 2 weeks, solid nodules were found at the inoculation site (~20 mm in size), indicating successful preparation of the rabbit tumor model. Rabbits were anesthetized with 3% (40 mg/kg) sodium pentobarbital for 20 min. Rabbits were euthanized by anesthesia followed by pentobarbital overdose. The experimental process was approved by the Medical Ethics Committee of the Jincheng Anthracitic Coal Mining Group General Hospital (Jincheng, China).

^{18}F -fluorodeoxyglucose (FDG) PET/CT imaging. PET/CT (Biography MCTs; Siemens AG) is a 52-ring, large aperture scanner. PET was performed using a three-dimensional (3D) collection mode with a layer thickness of 3.75 mm, a matrix of 128x128 and a collection rate of 3 min/bed. The CT acquisition conditions were as follows: Voltage, 120 kV; current, 200 mA; spiral time, 0.8 seconds/circles; bed speed, 22.5 mm/sec and matrix, 512x512. Image merging and management was performed using an Xeleris workstation (version 4.1; GE Healthcare). ^{18}F -FDG with a radiochemical purity >95% was provided by the PET/CT office at the Center of Jincheng Anthracitic Coal Mining Group General Hospital. VX_2 tumor model rabbits were fasted for 4-6 h and subsequently anesthetized with 3% (40 mg/kg) sodium pentobarbital before imaging. ^{18}F -FDG at 0.5 mCi/Kg was injected into the ear vein of the rabbits; PET/CT scanning was performed after 60 min. The tumor position was determined by PET/CT imaging and ^{125}I seeds (0.4 mCi or 0.7 mCi) were implanted at the tumor sites. PET/CT scans were performed again at 72 h and 2 and 4 weeks to obtain the tumor index, which included SUV and tumor length.

Particle implantation. The rabbits were implanted with 0.4 mCi ^{125}I seeds into the left hind leg, while 0.7 mCi seeds were implanted into the right hind leg. The implanting doses

were calculated using the Radiation Therapy Planning System (cat. no. KL-SIRPS-3D-800; Beijing ASTRO Technology Development Co., Ltd.).

Tumor inhibition rate assessment. The standard uptake values were measured using the Ellipsoid Isocontour 3D measurement method featured in the PET/CT software (PETViewer 2.0; Informer Technologies, Inc.), and the tumor lengths were measured on PET images. SUV=2.5 in the target area of the PET/CT image was set as the background deduction parameter to outline the region of interest (ROI). The ROI peak (1 cm³) was measured. SUV variation was calculated as follows: $\Delta\text{SUV}=(\text{SUV}_{\text{initial}}-\text{SUV}_{\text{final}})/\text{SUV}_{\text{initial}} \times 100\%$. Tumor inhibition rate was calculated as follows: $(\text{Tumor length}_{\text{initial}}-\text{tumor length}_{\text{final}})/\text{tumor length}_{\text{initial}} \times 100\%$.

Pathological observation. Each rabbit was sacrificed by pentobarbital overdose (injection of 100 mg/kg sodium pentobarbital) and two tumors in total, one from the left and one from the right leg, were harvested. The tumor tissue samples were selected from 5-10 mm around the ^{125}I seed region and obtained by tumor puncture. The removed tissue samples were fixed overnight in 10% neutral buffered formalin, embedded in paraffin, cut into 5- μm -thick sections, and placed on Superfrost Plus slides (Thermo Fisher Scientific, Inc.). Sections were subjected to hematoxylin staining for 5 min and eosin staining for 2 min at 20°C. For immunohistochemistry, deparaffinized and rehydrated slides using xylene and ethanol gradient, respectively, were subjected to antigen retrieval via autoclaving in a 10 mM citric acid buffer (pH 6.0). Upon cooling to room temperature for 30 min slides were blocked with 0.3% H_2O_2 for 20 min, washed in PBS, and then blocked with 1% BSA in PBS at 25°C. Slides were incubated with diluted primary antibodies Bax (1:200; cat. no. EL600961-100; EterLife) and Bcl-2 (1:150; cat. no. EL600995-100; EterLife) overnight at 4°C, and were subsequently incubated with diluted HRP-conjugated secondary goat anti-rabbit IgG antibody for 2 h at 37°C (1:500; cat. no. EL990003; EterLife). The expression levels of apoptosis-associated proteins Bcl-2 and Bax were detected based on the histology slide. The positive expression of Bcl-2 and Bax was identified as the precipitation of brown-yellow particles by IHC staining in the cytoplasm. A total of six high-power fields (magnification, x400) were randomly selected from each section and 200 cells were manually counted using a cell counter in each field to evaluate the percentage of tumor-positive cells. The expression intensities of Bcl-2 and Bax were measured according to the tumor-positive cells in the field of view and the ratio of Bcl-2 and Bax (Bcl-2/Bax) was evaluated.

Statistical analysis. The statistical analysis was conducted using SPSS 13.0 software (SPSS, Inc.). Data are presented as the mean \pm SD of three experimental repeats. Unpaired student's t-test was performed to compare tumor indexes, including tumor length, SUV and Bcl-2 and Bax expression in the left and right legs, before ^{125}I implantation. Spearman's correlation coefficients were calculated to evaluate the association between the average tumor length, Bcl-2, Bax and SUV. $P<0.05$ was considered to indicate a statistically significant difference. Following ^{125}I implantation, the association

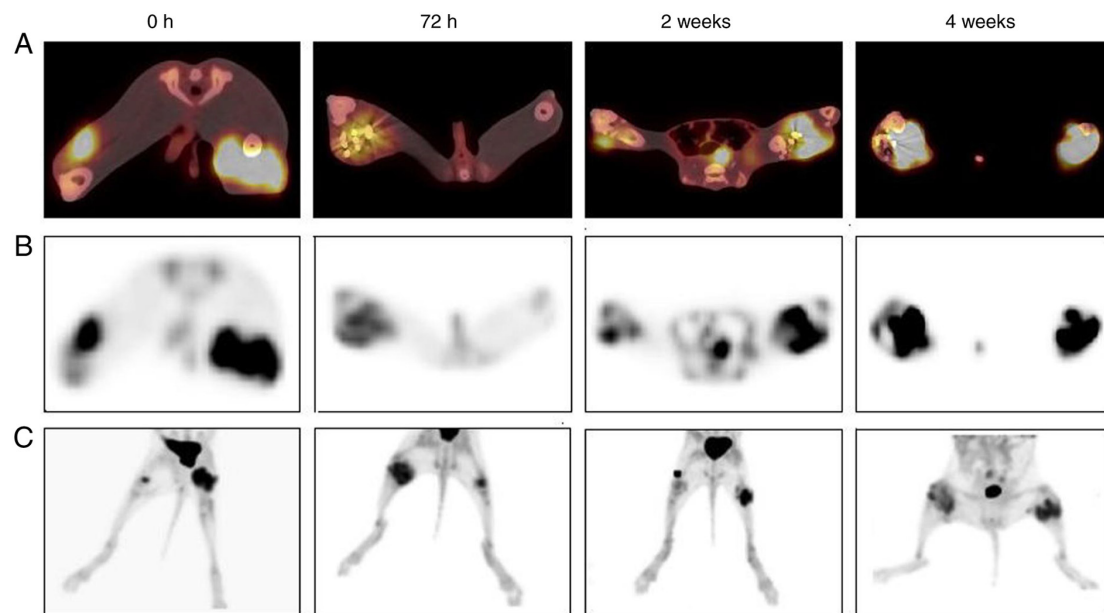


Figure 1. PET/CT and SUV images. (A) PET/CT and (B) SUV and (C) SUV images of two legs. PET/CT, positron emission tomography/computed tomography; SUV, standard uptake value.

between Δ SUV, tumor inhibition rate and Bcl-2/Bax in the 0.4 and 0.7 mCi ^{125}I groups was analyzed by IHC staining.

Results

Pathological observation. Following ^{125}I seed implantation, tumor cell proliferation, according to growth speed records (time taken by the cells to cover the entire culture dish, examined via semi-quantitative analysis; data not shown), decreased, necrotic areas appeared, peripheral fibrous connective tissue was destroyed and tumor angiogenesis decreased. PET/CT scans (Fig. 1A) showed that the metabolic rate and volume of tumor tissue decreased over time. Following ^{125}I seed implantation, liquefactive necrotic areas gradually appeared in the center of the tumor tissue (showing no metabolic signals) and the necrotic area was notably large (Fig. 1B and C).

The results of HE staining (Fig. 2) showed that, following ^{125}I seed implantation, the tumor tissue demonstrated notable liquefaction of the necrotic areas. Furthermore, the number of tumor cells notably decreased and the surrounding fibrous connective tissue was extensively destroyed. Compared with the 0.4 mCi group, the proliferation signal of tumor cells in the 0.7 mCi group decreased more notably, which indicated that there were fewer tumor cells following implantation of 0.7 mCi ^{125}I .

Tumor index results. Bcl-2 and Bax expression levels were observed via immunohistochemistry (Fig. 3). The expression intensity of Bcl-2 decreased over time, while the expression intensity of Bax increased, which indicated that apoptosis increased during treatment.

Fig. 4 shows the statistical tumor index results, including the mean \pm SD tumor length, SUV and Bcl-2 and Bax intensity before and after ^{125}I implantation. Before treatment, t-test showed no significant difference in the distribution of the tumor length and SUV in the left and right legs. Following

treatment, the mean tumor length and SUV in both groups decreased. At 2 and 4 weeks, SUV was significantly decreased. For both groups, a significant decrease in the average SUV was observed at 2 weeks after treatment, while it was more pronounced in the 0.7 mCi group (Fig. 4B). Following implantation, Bcl-2 expression decreased and Bax expression increased (Fig. 4C and D). In addition, the decrease of Bcl-2 in the 0.7 mCi group was larger than that in the 0.4 mCi group. Bcl-2 expression continuously decreased over 4 weeks. By contrast, the increase of Bax in the 0.7 mCi group was higher than that of the 0.4 mCi group. These quantitative data demonstrated that the treatment was effective and that 0.7 mCi ^{125}I seeds were more effective as a tumor therapy compared with 0.4 mCi seeds.

Fig. 5 presents the association between variations in tumor indexes, including Δ SUV, tumor inhibition rate and Bcl-2/Bax at different time points following ^{125}I implantation. At 72 h, Δ SUV, tumor inhibition rate and Bcl-2/Bax data were relatively dispersed. The data became concentrated as the time elapsed from 2 to 4 weeks. These results indicated that the effect of each implantation varied greatly at the beginning but after 4 weeks, all 30 rabbits demonstrated similar treatment effects. Meanwhile, in the 0.7 mCi group, each tumor index indicator showed a better distribution (smaller intragroup differences) in data analysis, which also indicated that 0.7 mCi ^{125}I seeds held greater therapeutic potential in terms of treatment effect.

Discussion

Since the 1960s, research on permanent intertissue implantation of radioactive particles for the treatment of malignant tumors has demonstrated notable advancements (22,23). However, there is currently no uniform dose standard for ^{125}I seeds, which is the most widely used therapeutic radioactive particle for permanent intertissue implantation in clinical practice, particularly for solid tumor therapy. Its half-life is

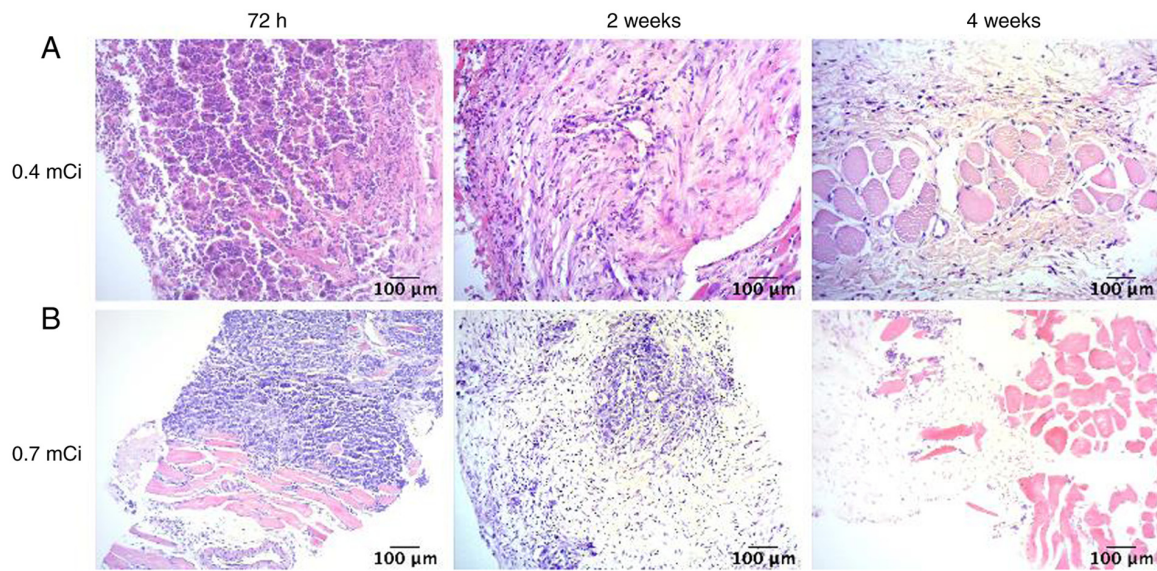


Figure 2. Hematoxylin and eosin staining. ^{125}I seeds were implanted at (A) 0.4 and (B) 0.7 mCi.

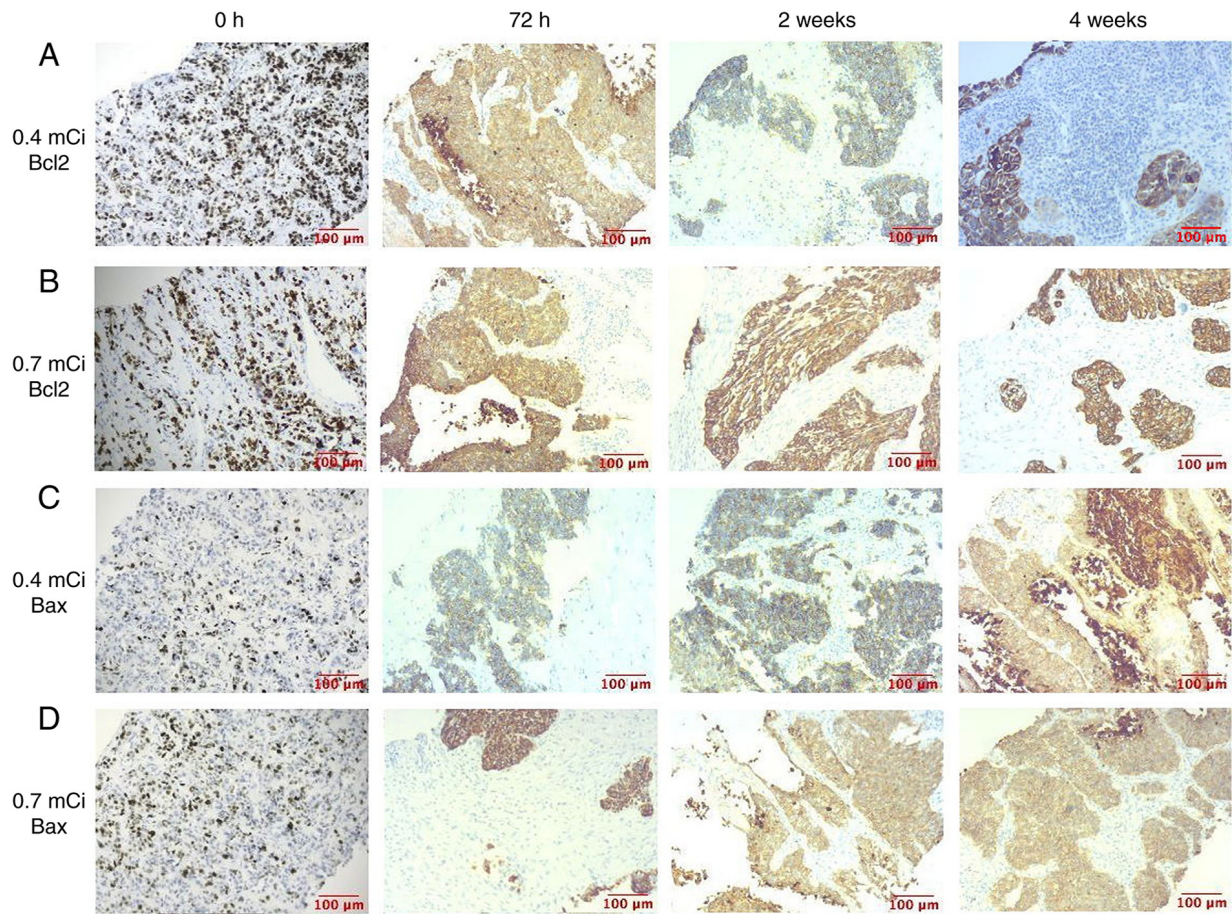


Figure 3. Immunohistochemistry of Bcl-2 and Bax. Bcl-2 expression following implantation of (A) 0.4 and (B) 0.7 mCi ^{125}I seeds. Bax expression following implantation of (C) 0.4 and (D) 0.7 mCi ^{125}I seeds.

59.49 days and it decays by electron capture to an excited state of ^{125}Te . This state is not the metastable $^{125\text{m}}\text{Te}$, but rather a lower energy state that decays immediately by gamma decay with a maximum energy of 35 keV. The state of low energy makes it possible for tumor treatment for its appropriate effects,

such as fewer side effects and more treatment effects (22,23). To determine the optimal standard dose of ^{125}I seeds for solid tumor therapy and provide a theoretical basis for the optimal clinical application of radioactive particles such as ^{125}I seeds, the present study used New Zealand White rabbits

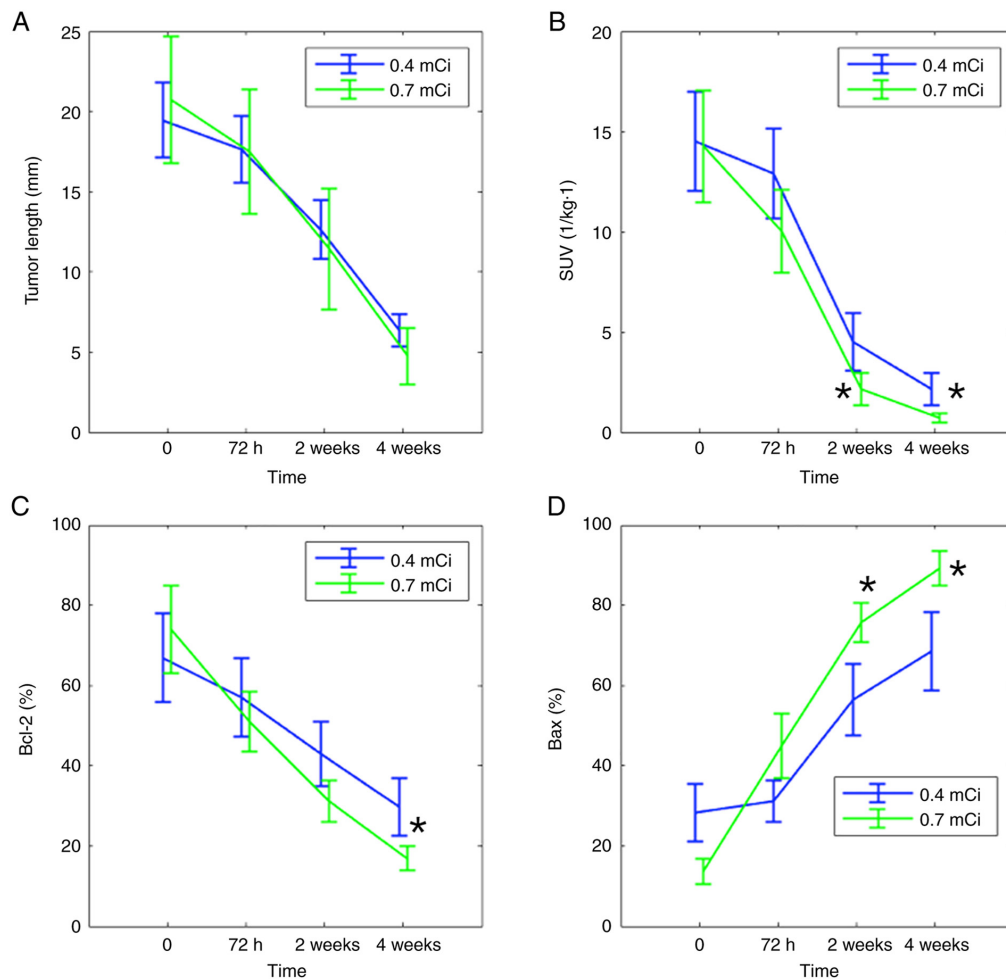


Figure 4. Tumor indexes before and after ^{125}I implantation. (A) Tumor length. (B) SUV. (C) Bcl-2 expression intensity. (D) Bax expression intensity. SUV and Bcl-2 expression were significantly lower and Bax expression was significantly higher in the 0.7 mCi group after 4 weeks. SUV, standard uptake value. * $P < 0.05$ vs. 0.4 mCi.

to construct a VX_2 solid tumor xenograft model in the hind leg. Theoretically, ^{125}I seeds do not affect the SUV of PET/CT, because they have distinct mechanisms. PET provides detailed information about the function and metabolism of the tumor lesion. PET/CT image-guided surgery utilizes ^{18}F -FDG to monitor the biochemical activity of the tumor (24,25). ^{125}I seeds at 0.4 mCi were implanted into the left hind leg and ^{125}I seeds at 0.7 mCi into the right hind leg of each rabbit. Changes in tumor length, SUV and the ratio of Bcl-2/Bax were compared before and after ^{125}I seed implantation by PET/CT scans to assess the therapeutic effect of ^{125}I seeds on solid tumors. Using comparative analysis, it was shown that, compared with ^{125}I seeds at 0.4 mCi activities, treating solid tumors with ^{125}I seeds with 0.7 mCi activity exhibited a more obvious therapeutic effect, as demonstrated by decreased tumor length, SUV and Bcl-2 expression and increased Bax following treatment. ^{125}I seeds at 0.7 mCi activity resulted in a more consistent treatment effect, which indicated that ^{125}I seeds at 0.7 mCi may be more beneficial in clinical applications.

There is controversy surrounding the effect of ^{125}I seed implantation at different activity levels and durations for solid tumor treatment, for which there is no unified standard for comparative analysis. To the best of our knowledge, there are

few literature reports on the safety of ^{125}I seeds at different activity levels in the treatment of solid tumors. Therefore, upper and lower prescription doses have not been established for solid tumor treatment using radioactive ^{125}I seeds in terms of interstitial implantation.

Several studies have reported that different doses of ^{125}I seeds implanted into tissue have different effects on tumor eradication (26-28). In the present study, ^{125}I seeds with 0.7 mCi activity caused tumors to shrink in a short period of time, while ^{125}I seeds with 0.4 mCi activity did not completely inhibit tumor growth.

With respect to the comprehensive and periodic treatment of solid tumors, the selection of ^{125}I seeds with 0.7 mCi activity is more consistent with results previously reported by Wang *et al* (29), who found that low-activity particles had a lower dose inhibition rate for tumor tissues compared with high-activity particles, and that the radiation released by the particles decayed rapidly with increasing distance. Thus, low-activity radioactive particles do not completely inhibit the proliferation of tumor tissue, unless very high doses are selected in clinical practice. However, increasing the dosage of low-activity particles in the treatment of solid tumors results in greater potential for tumor radiotherapy side effects, such as the damage of normal tissues (30). Pan *et al* found that

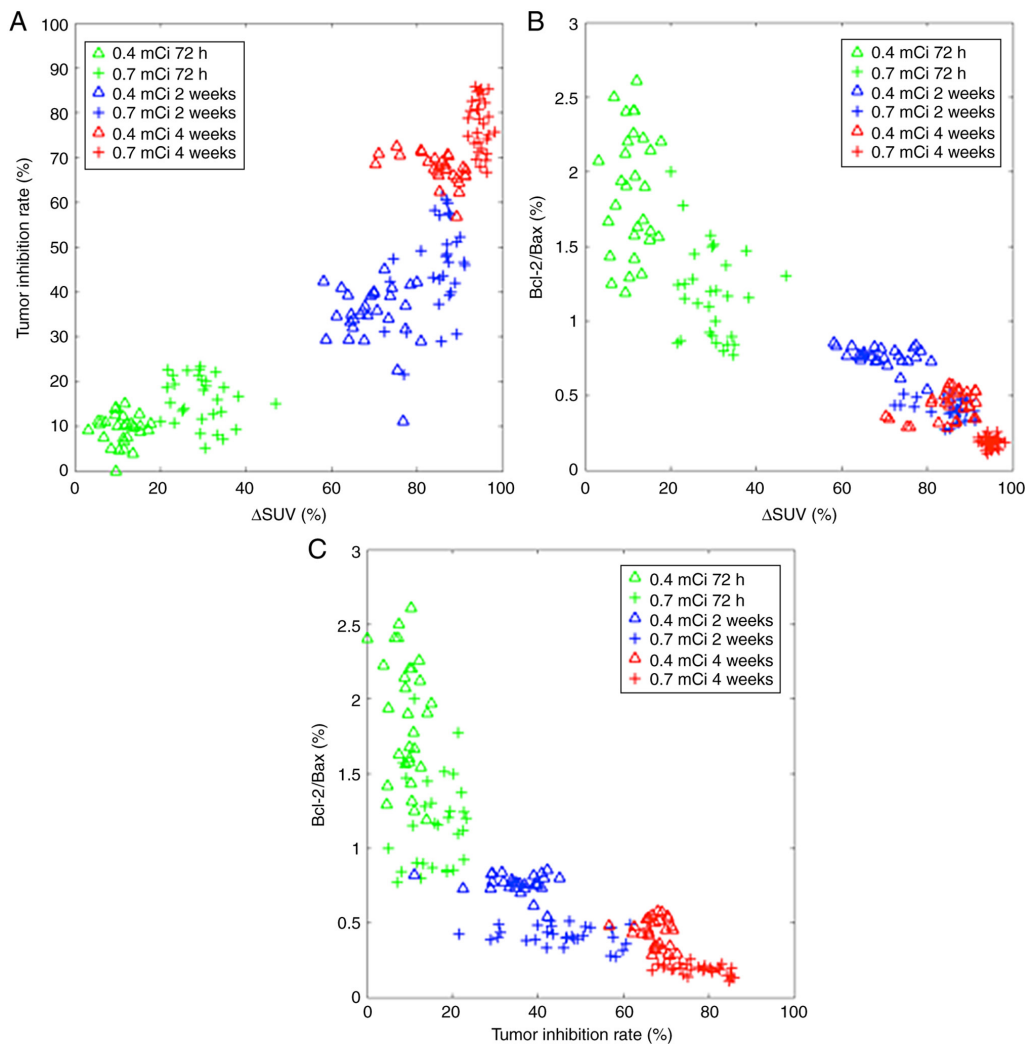


Figure 5. Bcl-2/Bax and tumor inhibition rate. Association between (A) tumor inhibition rate and ΔSUV ($r=0.9570$; $P=0.0430$), (B) Bcl-2/Bax and ΔSUV ($r=0.9717$; $P=0.0283$) and (C) Bcl-2/Bax and tumor inhibition rate ($r=-0.9943$; $P=0.0057$). SUV, standard uptake value; w, weeks.

^{32}P -CP-PLLA particles significantly inhibit the glucose metabolism of VX_2 tumors, thereby promoting tumor cell apoptosis. They also confirmed the association between tumor SUV metabolism and radioactive particle dose (31). The present results showed that most tumor cells were necrotic after using ^{125}I seeds to treat VX_2 tumors; there was no metabolic signal in the treatment area and the number of active tumor cells decreased. Following treatment of VX_2 solid tumor xenografts with ^{125}I seeds for 72 h, PET/CT (which can detect morphological changes of VX_2 solid tumors) was used to evaluate the therapeutic effect of ^{125}I seeds on solid tumors. Through comparative analysis of changes in tumor length, SUV and the expression of molecules associated with tumor metabolism, such as Bcl-2 and Bax, the present study demonstrated that the therapeutic effect of 0.7 mCi ^{125}I seeds was better than that of 0.4 mCi ^{125}I seeds.

Through immunohistochemical staining and pathological observation, the present study showed that ^{125}I radioactive seeds participate in the apoptosis of tumor cells by regulating expression of tumor metabolism-associated molecules, such as Bcl-2 and Bax, to inhibit solid tumor growth. The ratio of Bcl-2/Bax expression was notably downregulated following treatment. More importantly, there was a correlation between

decreased Bcl-2/Bax expression content ratio and activity of radioactive ^{125}I seeds, indicating that, compared with 0.4 mCi ^{125}I seeds, 0.7 mCi ^{125}I seeds exhibited a better therapeutic effect on solid tumors. The present study observed the short-term therapeutic effects of 0.4 mCi and 0.7 mCi ^{125}I radioactive seeds VX_2 solid tumors. Additionally, there were no adverse effects in either treatment group. This is consistent with studies that 0.7 mCi seed activity is commonly used and dosage as high as 0.8-2.5 mCi is safe (32-37).

The present study had certain limitations. First, this was a paired comparison and further studies should compare differences between groups using more samples. Experiments should be performed using the left leg as a control with 0 mCi seeds and implanting the right leg with 0.7 or 0.4 mCi ^{125}I seeds to demonstrate the therapeutic effect of each activity level. The 4-week therapeutic effects of ^{125}I seeds on solid tumors are still unknown. In addition, the small number of experimental groups, as well as the small sample size, may lead to biased conclusions. In future, the 4-week therapeutic effects of ^{125}I seeds of different activity levels in the treatment process of solid tumors should be studied. Future investigations should increase the number of experimental groups and sample size to generate high-quality research data.

In conclusion, low-activity ^{125}I implantation was effective for VX_2 tumor treatment and 0.7 mCi ^{125}I seeds may be more suitable in the clinic than 0.4 mCi seeds.

Acknowledgements

Not applicable.

Funding

The present study was supported by Scientific Research Projects of Shanxi Health Commission (grant no. 2018139).

Availability of data and materials

The datasets used and/or analyzed during the current study are available from the corresponding author on reasonable request.

Authors' contributions

YY, ZW, JW, FW, QF and RZ participated in study conception and design, performed the experiments and analyzed/interpreted data. ZW, JW and RZ confirm the authenticity of all the raw data. All authors have read and approved the final manuscript.

Ethics approval and consent to participate

The present study was approved by Jincheng Anthracitic Coal Mining Group General Hospital (approval no. 2018139; Jincheng, China).

Patient consent for publication

Not applicable.

Competing interests

The authors declare that they have no competing interests.

References

- Cheng J, Ma S, Yang G, Wang L and Hou W: The mechanism of computed tomography-guided ^{125}I particle in treating lung cancer. *Med Sci Monit* 23: 292-299, 2017.
- Lin L, Wang J, Jiang Y, Meng N, Tian S, Yang R, Ran W and Liu C: Interstitial ^{125}I seed implantation for cervical lymph node recurrence after multimodal treatment of thoracic esophageal squamous cell carcinoma. *Technol Cancer Res Treat* 14: 201-207, 2015.
- Gaopeng L, Shengli D, Ye LU, Miaoyun L, Jian G and Qibin T: The cooperative effect of p53 and Rb in local nanotherapy in a rabbit VX_2 model of hepatocellular carcinoma. *Int J Nanomedicine* 8: 3757-3768, 2013.
- Leth T, Von Oettingen G, Lassen-Ramshad YA, Lukacova S and Høyer M: Survival and prognostic factors in patients treated with stereotactic radiotherapy for brain metastases. *Acta Oncologica* 54: 107-114, 2015.
- Quintás-Cardama A, Daver N, Kim H, Dinardo C, Jabbour E, Kadia T, Borthakur G, Pierce S, Shan J, Cardenas-Turan M, *et al*: A prognostic model of therapy-related myelodysplastic syndrome for predicting survival and transformation to acute myeloid leukemia. *Clin Lymphoma Myeloma Leukemia* 14: 401-410, 2014.
- Třeška V, Duras P, Mírka H, Skalický T and Sutnar A: [Chemoembolization with Drug Eluting Beads (TACE DEB) in patients with primary unresectable hepatocellular carcinoma (HCC)]. *Rozhledy v chirurgii: měsíčník eskoslovenské chirurgické společnosti* 93: 63-69, 2014.
- Hutchings M: FDG-PET response-adapted therapy: Is ^{18}F -fluorodeoxyglucose positron emission tomography a safe predictor for a change of therapy? *Hematol Oncol Clin North Am* 28: 87-103, 2014.
- Lim AJ, Brandon AH, Fiedler J, Brickman AL, Boyer CI, Raub WA Jr and Soloway MS: Quality of life: Radical prostatectomy versus radiation therapy for prostate cancer. *J Urol* 154: 1420-1425, 1995.
- Gao F, Li C, Gu Y, Huang J and Wu P: CT-guided ^{125}I brachytherapy for mediastinal metastatic lymph nodes recurrence from esophageal carcinoma: Effectiveness and safety in 16 patients. *Eur J Radiol* 82: e70-e75, 2013.
- Nakamura R, Kikuchi K, Tanji S, Yabuuchi T, Uwano I, Yamaguchi S, Ariga H and Fujioka T: Narrow safety range of intraoperative rectal irradiation exposure volume for avoiding bleeding after seed implant brachytherapy. *Radiat Oncol* 7: 15, 2012.
- Zhang F, Wu K, Gao F, Zhang W, Shi F and Li C: Refractory nasopharyngeal carcinoma: Positron emission tomography combined with computed tomography-guided ^{125}I seed implantation therapy after repeated traditional radiochemotherapy. *Otolaryngol Head Neck Surg* 149: 417-423, 2013.
- Li C, Yao L, Gong J, Pang H, Shan Q, Wang Z, Lu J and Wang Z: Efficacy of gefitinib combined with ^{125}I radioactive particles in the treatment of transplanted lung cancer tumors in nude mice. *Cardiovasc Intervent Radiol* 43: 1364-1370, 2020.
- Toba H, Sakiyama S, Otsuka H, Kawakami Y, Takizawa H, Kenzaki K, Kondo K and Tangoku A: ^{18}F -fluorodeoxyglucose positron emission tomography/computed tomography is useful in postoperative follow-up of asymptomatic non-small-cell lung cancer patients. *Interact Cardiovasc Thorac Surg* 15: 859-864, 2012.
- Zou JF: Effect of ^{125}I radioactive particle implantation combined with TACE treatment on serum markers apoptotic molecules in tumor tissue of patients with primary hepatocellular carcinoma. *J Hainan Medical University* 22: 101-104, 2016.
- Lu KV, Chang JP, Parachoniak CA, Pandika MM, Aghi MK, Meyronet D, Isachenko N, Fouse SD, Phillips JJ, Cheresch DA, *et al*: VEGF inhibits tumor cell invasion and mesenchymal transition through a MET/VEGFR2 complex. *Cancer Cell* 22: 21-35, 2012.
- Aggarwal S, Devaraja K, Sharma SC and Das SN: Expression of vascular endothelial growth factor (VEGF) in patients with oral squamous cell carcinoma and its clinical significance. *Clinica Chimica Acta* 436: 35-40, 2014.
- Li M, Wang Z, Xing Y, Yu J, Tian L, Zhang D and Xin Z: A multicenter study on expressions of vascular endothelial growth factor, matrix metalloproteinase-9 and tissue inhibitor of metalloproteinase-2 in oral and maxillofacial squamous cell carcinoma. *Iran Red Crescent Med J* 16: e13185, 2014.
- Diaz-Rubio E, Gomez-Espana A, Massuti B, Sastre J, Abad A, Valladares M, Rivera F, Safont MJ, Martínez de Prado P, Gallén M, *et al*: First-line XELOX plus bevacizumab followed by XELOX plus bevacizumab or single-agent bevacizumab as maintenance therapy in patients with metastatic colorectal cancer: The phase III MACRO TTD study. *Oncologist* 17: 15-25, 2012.
- Verma A, Um SW, Koh WJ, Suh GY, Chung MP, Kwon OJ and Kim H: Long-term tolerance of airway silicone stent in patients with post-tuberculosis tracheobronchial stenosis. *ASAIO J* 58: 530-534, 2012.
- Dedic-Hagan J, Teh AY, Liang E, Collett N and Woo HH: Migration of a strand of four seeds in low-dose-rate brachytherapy. *BMJ Case Rep*: May 30, 2014 (Epub ahead of print). doi: 10.1136/ber-2014-204515.
- Shin DY, Han SW, Oh DY, Im SA, Kim TY and Bang YJ: Prognostic implication of ^{18}F FDG-PET in patients with extrahepatic metastatic hepatocellular carcinoma undergoing systemic treatment, a retrospective cohort study. *Cancer Chemother Pharmacol* 68: 165-175, 2011.
- Salem R, Gordon AC, Mouli S, Hickey R, Kallini J, Gabr A, Mulcahy MF, Baker T, Abecassis M, Miller FH, *et al*: Y90 radioembolization significantly prolongs time to progression compared with chemoembolization in patients with hepatocellular carcinoma. *Gastroenterology* 151: 1155-1163.e2, 2016.

23. Assi R, Kantarjian H, Ravandi F and Daver N: Immune therapies in acute myeloid leukemia: A focus on monoclonal antibodies and immune checkpoint inhibitors. *Curr Opin Hematol* 25: 136-145, 2018.
24. Caresia Aroztegui AP, Garcia Vicente AM, Alvarez Ruiz S, Delgado Bolton RC, Orcajo Rincon J, Garcia Garzon JR, de A rcocha Torres M and Garcia-Velloso MJ: Oncology Task Force of the Spanish Society of Nuclear Medicine and Molecular Imaging: 18F-FDG PET/CT in breast cancer: Evidence-based recommendations in initial staging. *Tumour Biol*: Oct 12, 2017 (Epub ahead of print). doi: 10.1177/1010428317728285.
25. Dietlein M, Klusmann JP and Drzezga A: 18F-FDG PET/CT in head and neck tumors. *Nuklearmedizin* 59: 8-11, 2020 (In German).
26. Wang H, Peng R, Li X, Wang Y, Jiang Y, Ji Z, Guo F, Tian S, Sun H, Fan J and Wang J: The dosimetry evaluation of 3D printing non-coplanar template-assisted CT-guided 125I seed stereotactic ablation brachytherapy for pelvic recurrent rectal cancer after external beam radiotherapy. *J Radiat Res* 62: 473-482, 2021.
27. Qu A, Jiang P, Wei S, Jiang Y, Ji Z, Sun H, Li W, Shao Y, Fan J and Wang J: Accuracy and dosimetric parameters comparison of 3D-printed non-coplanar template-assisted computed tomography-guided iodine-125 seed ablative brachytherapy in pelvic lateral recurrence of gynecological carcinomas. *J Contemp Brachytherapy* 13: 39-45, 2021.
28. Li J, Wang J, Meng N, Qu A, Yuan H, Liu C, Ran W and Jiang Y: Image-guided percutaneous (125)I seed implantation as a salvage treatment for recurrent soft tissue sarcomas after surgery and radiotherapy. *Cancer Biother Radiopharm* 26: 113-120, 2011.
29. Wang W, Qin H, Zhu X, *et al*: The study of different activity ~(125)I seeds implantation to therapy rabbit liver VX2 tumor. *Journal of Anhui Medical University* 50: 778-781 2015 (In Chinese).
30. Bradley JD, Paulus R, Komaki R, Masters G, Blumenschein G, Schild S, Bogart J, Hu C, Forster K, Magliocco A, *et al*: Standard-dose versus high-dose conformal radiotherapy with concurrent and consolidation carboplatin plus paclitaxel with and without cetuximab for patients with stage IIIA and IIIB non-small-cell lung cancer (RTOG 0617): A randomized, two-by-two factorial phase 3 study. *Lancet Oncol* 16: 187-199, 2015.
31. Pan D, Yang M, Xu Y, Wang L, Liu L and Huang P: Experimental study of CT guided ³²P-CP-PLLA microparticle implantation in the treatment of rabbit VX2 lung tumor. *Zhongguo Fei Ai Za Zhi* 14: 1-6, 2011 (In Chinese).
32. He X, Liu M, Zhang M, Sequeiros RB, Xu Y, Wang L, Liu C, Wang Q, Zhang K and Li C: A novel three-dimensional template combined with MR-guided (125)I brachytherapy for recurrent glioblastoma. *Radiat Oncol* 15: 146, 2020.
33. Li CC, Chi JL, Ma Y, Li JH, Xia CQ, Li L, Chen Z and Chen XL: Interventional therapy for human breast cancer in nude mice with 131I gelatin microspheres (¹³¹I-GMSs) following intratumoral injection. *Radiat Oncol* 9: 144, 2014.
34. Zhao GS, Liu S, Yang L, Li C, Wang RY, Zhou J and Zhang YW: Evaluation of radioactive (125)I seed implantation for the treatment of refractory malignant tumours based on a CT-guided 3D template-assisted technique: Efficacy and safety. *BMC Cancer* 20: 718, 2020.
35. Yao LH, Su L, Liu L, Sun HT and Wang JJ: Stenting of the portal vein combined with different numbers of Iodine-125 seed strands: Dosimetric analyses. *Chin Med J (Engl)* 130: 2183-2189, 2017.
36. Huo X, Huo B, Wang H, Wang L, Cao Q, Zheng G, Wang J, Chai S, Zhang Z, Yang K, *et al*: Implantation of computed tomography-guided Iodine-125 seeds in combination with chemotherapy for the treatment of stage III non-small cell lung cancer. *J Contemp Brachytherapy* 9: 527-534, 2017.
37. Yang Z, Zhang Y, Xu D, Maccauro G, Rossi B, Jiang H, Wang J, Sun H, Xu L, Chen Y and Liu X: Percutaneous vertebroplasty combined with interstitial implantation of 125I seeds in banna mini-pigs. *World J Surg Oncol* 11: 46, 2013.



This work is licensed under a Creative Commons Attribution-NonCommercial-NoDerivatives 4.0 International (CC BY-NC-ND 4.0) License.